Tissue-specific calibration of extracellular matrix material properties by transforming growth factor-beta and Runx2 in bone is required for hearing

Chang, JL; Brauer, DS; Johnson, J; Chen, CG; Akil, O; Balooch, G; Humphrey, MB; Chin, EN; Porter, AE; Butcher, K; Ritchie, RO; Schneider, RA; Lalwani, A; Derynck, R; Marshall, GW; Marshall, SJ; Lustig, L; Alliston, T

Tissue-specific calibration of extracellular matrix material properties by transforming growth factor-b and Runx2 in bone is required for hearing

Jolie L. Chang[1], Delia S. Brauer[2], Jacob Johnson[1], Carol Chen[3], Omar Akil[1], Guive Balooch[4,5], Mary Beth Humphrey[6], Emily N. Chin[3], Alexandra E. Porter[7], Kristin Butcher[3], Robert O. Ritchie[4,5], Richard A. Schneider[3,8], Anil Lalwani[9], Rik Derynck[8,10], GraysonW.Marshall[2], Sally J. Marshall[2], Lawrence Lustig[1] & Tamara Alliston[1,3,8,11+]

[1]Department of Otolaryngology and Head and Neck Surgery, [2]Department of Preventive and Restorative Dental Sciences, and [3]Department of Orthopaedic Surgery,University of California, San Francisco, California, USA, [4]Department of Materials Science and Engineering, University of California, [5]Materials Science Division, Lawrence Berkeley National Laboratories, Berkeley, California, USA, [6]Department of Medicine and Microbiology/Immunology, University of Oklahoma Health Science Center, Oklahoma City, Oklahoma, USA, [7]Materials, Imperial College, London, UK, [8]Institute for Regeneration Medicine, [9]Department of Cell and Tissue Biology, and [10]Department of Bioengineering and Therapeutic Sciences, University of California, San Francisco, San Francisco, California, USA, and [11]Department of Otolaryngology, New York University, New York, USA

ABSTRACT

Physical cues, such as extracellular matrix stiffness, direct cell differentiation and support tissue-specific function. Perturbation of these cues underlies diverse pathologies, including osteoarthritis, cardiovascular disease and cancer. However, the molecular mechanisms that establish tissue-specific material properties and link them to healthy tissue function are unknown. We show that Runx2, a key lineage-specific transcription factor, regulates the material properties of bone matrix through the same transforming growth factor-b (TGFβ)-responsive pathway that controls osteoblast differentiation. Deregulated TGFβ or Runx2 function compromises the distinctly hard cochlear bone matrix and causes hearing loss, as seen in human cleidocranial dysplasia. In $Runx2^{+/-}$ mice, inhibition of TGFβ signalling rescues both the material properties of the defective matrix, and hearing. This study elucidates the unknown cause of hearing loss in cleidocranial dysplasia, and demonstrates that a molecular pathway controlling cell differentiation also defines material properties of extracellular matrix. Furthermore our results suggest that the careful regulation of these properties is essential for healthy tissue function.

INTRODUCTION

Tissues have characteristic material properties that arise largely from their extracellular matrices (ECMs), ranging from stiff bone and enamel (approximately 107 kPa) to compliant brain and skin (approximately 0.1–250 kPa). In addition to their structural roles, the material properties of an ECM are powerful determinants of cell function. Similarly to biochemical signals, properties such as the elastic modulus direct cell differentiation and gene expression. Conversely, subtle changes in material properties of a tissue's ECM disrupt cell proliferation and drive disease progression (Butcher et al, 2009). Mechanisms that regulate ECM material properties are, therefore, important in development and disease, but very little is known about these mechanisms, or the functional roles of ECM material properties in healthy tissues.

The skeleton is an ideal model system in which to define mechanisms that establish ECM material properties and to understand their relationship with tissue-specific function. Healthy bone exhibits a variety of material properties depending on its skeletal location (Currey, 1999). Furthermore, factors that regulate ECM material properties were first discovered in the skeleton, including transforming growth factor-β (TGFβ). Alteration of TGFβ signalling in mice severely disrupts bone mass and the material properties of bone matrix (Balooch et al, 2005)—including elastic modulus and hardness—which determine the ability of bone matrix to resist deformation. Although the effects of TGFβ on bone mass are due to its regulation of osteoblasts and osteoclasts (Mohammad et al, 2009), the cellular and molecular targets of TGFb in the control of bone matrix material properties are not known.

TGFβ regulates osteoblast differentiation by targeting the lineage-specific transcription factor Runx2. In vitro, TGFβ represses Runx2 expression and function through a Smad3-dependent pathway that is essential for TGFβ to inhibit osteoblast differentiation (Alliston et al, 2001). The fact that TGFβ also represses Runx2 function in vivo is supported by the appearance of dysplastic clavicles and open cranial sutures in both $Runx2^{+/-}$ mice and in mice that overexpress TGFβ2 in osteoblasts (Erlebacher & Derynck, 1996; Otto et al, 1997). These are characteristics of the human genetic bone syndrome cleidocranial dysplasia (CCD), which results from RUNX2 haploinsufficiency (Cooper et al, 2001).

Patients with CCD also exhibit hearing loss (Visosky et al, 2003). Hearing loss in human CCD can be sensorineural (SNHL), conductive (CHL) or mixed. CHL occurs when sound cannot reach the cochlea in the inner ear due to problems in the external ear, tympanic membrane or middle ear. By contrast, SNHL results from cochlear, auditory nerve or central nervous system (CNS) defects. In many bone diseases, however, these clinical definitions blur, as in CCD, cochlear otosclerosis, Paget disease and osteogenesis imperfecta (Chole & McKenna, 2001; Hartikka et al, 2004; Monsell, 2004). For example, some cochlear otosclerosis patients exhibit SNHL without obvious damage to the organ of Corti or auditory nerve. Although these diseases highlight a role for bone in normal cochlear function, the mechanisms by which bone abnormalities cause SNHL are poorly understood.

Owing to its specialized structure and function, cochlear bone presents a unique opportunity to study the regulation and role of bone matrix properties. Cochlear bone is protected from normal bone remodelling (Sorensen, 1994) and has been suggested to be the hardest bone in the body, although this assertion is based on clinical experience and intriguing studies of whale ear bone (Currey, 1999). Thus, we hypothesize that the matrix properties of cochlear bone are precisely calibrated and required for normal hearing. To test this hypothesis, we

evaluated bone matrix material properties and hearing in two mouse models of CCD, namely Runx2þ/ mice and D4 mice with increased TGFβ expression in osteoblasts. This study has broad implications for other tissues it allows exploration of the mechanisms by which tissue-specific ECM material properties are established and linked to healthy tissue function.

RESULTS AND DISCUSSION

Bone matrix material properties are anatomically distinct

Although mouse models provide powerful tools with which to investigate the control of ECM material properties, most mouse bones are too small for macromechanical analyses. Nanoindentation measures material properties in the sub-micrometre range independently of bone size, porosity or shape (Rho et al, 1997). Using nanoindentation, we observed significant differences in the matrix elastic modulus of several mouse bones, ranging from the 30-GPa cochlear bone matrix to the 14-GPa calvarial bone matrix (Fig 1A). These data conclusively show that the cochlear capsule and ossicles are stiffer than other bones—as has been postulated previously (Currey, 1999)—and that ECM material properties depend on the anatomical identity of the bone.

Increased TGFb disrupts the unique material properties of cochlear bone and hearing

How are such differences in ECM material properties established and maintained? We previously identified TGFβ as a key regulator of bone matrix material properties (Balooch et al, 2005), but whether TGFβ also regulates bone quality in the unusual cochlear bone was unknown. Nanoindentation was used to evaluate cochlear bone from D4 mice that express an activated form of human TGFβ2 in osteoblasts under the control of osteocalcin promoter (Erlebacher & Derynck, 1996). The D4 cochlear bone matrix had decreased elastic modulus and hardness (Fig 1B,C), despite the lack of bone remodelling in the cochlea (Sorensen, 1994).

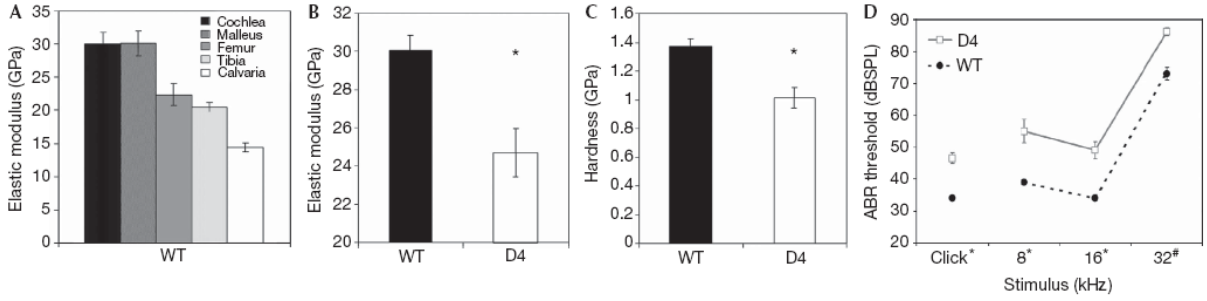

Fig 1 Transforming growth factor-β overexpression disrupts cochlear bone matrix material properties and hearing. (A) The elastic modulus (GPa) of each bone is distinct. In the otic capsule, the (B) elastic modulus and (C) hardness of D4 cochlear bone matrix are reduced relative to WT ($^{*}P<0.01$). (D) D4 mice (open squares) have elevated ABR thresholds for click and pure tone stimuli relative to WT (filled circles) ($^{*}P<0.001$; $^{\#}P<0.005$). All error bars represent s.d. values. ABR, auditory brainstem response; TGFβ, transforming growth factor-β; WT, wild type.

Presumably, tissue-specific material properties arise under selective pressure. Their functional importance has long been suggested (Currey, 1999), but is difficult to discern independently from other aspects of bone quality. To determine whether the decrease in cochlear bone hardness in D4 mice compromised cochlear function, we tested hearing in D4 and wild-type (WT) mice using the auditory brainstem response (ABR). An elevated auditory threshold, the lowest volume that elicits an ABR, indicates hearing loss. Stimuli included a multi-frequency click and pure tones at 8, 16 and 32 kHz. The D4 mice had significantly elevated ABR thresholds

compared with WT (Fig 1D), with mean differences ranging from 13 to 16 dB. Therefore, increased TGFβ signalling in bone impaired both the material properties of cochlear bone and hearing, suggesting that the unique material properties of this tissue might be required for function.

Runx2 insufficiency impairs hearing

These observations raised two key questions. First, are defective bone matrix material properties responsible for hearing loss in D4 mice or in human disease? Second, what are the mechanisms by which TGFβ defines matrix material properties and hearing? A major clue came from the fact that both D4 and Runx2$^{+/-}$ mice have characteristics of CCD; a syndrome linked to loss of Runx2 function (Fig 2A). Another feature of human CCD is hearing loss (Cooper et al, 2001; Visosky et al, 2003), although hearing in Runx2$^{+/-}$ mice has not been evaluated. In this study, we observed that Runx2$^{+/-}$ mice have significantly higher ABR thresholds than WT mice (Fig 2B), similar to D4 mice. Compound action potentials (CAPs) were recorded to discriminate involvement of the CNS in hearing loss. The elevated CAP thresholds in Runx2$^{+/-}$ mice revealed that the CNS is not involved, thereby isolating hearing loss to the peripheral auditory system (Fig 2C).

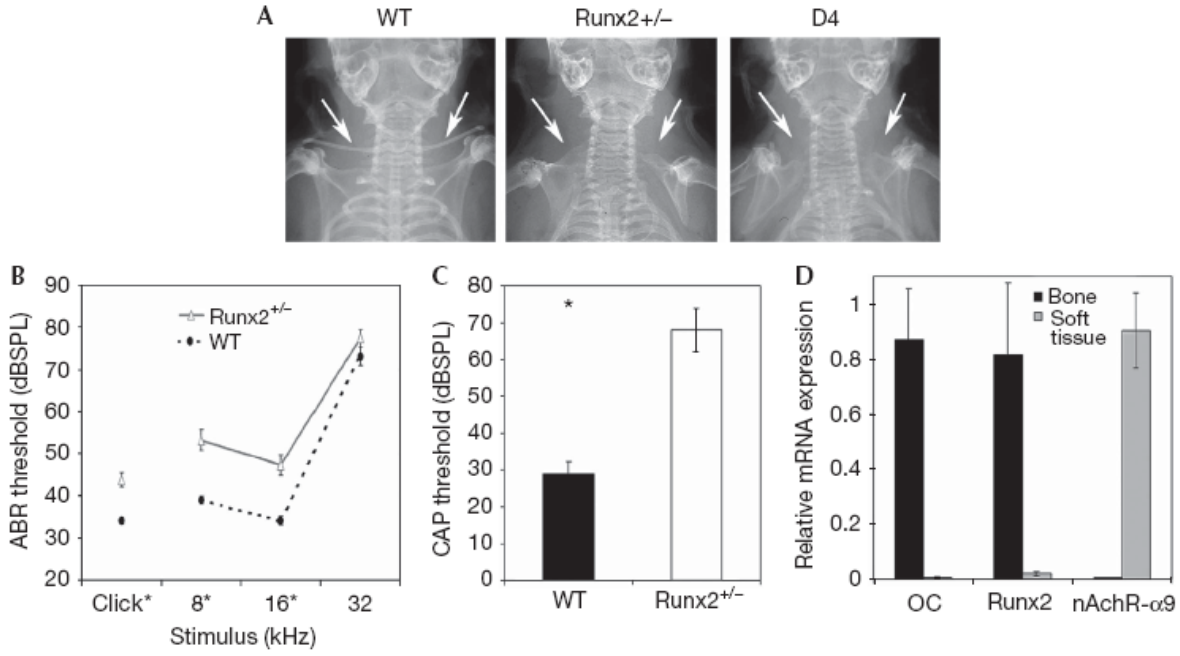

Fig 2 Runx2 insufficiency in mouse models of cleidocranial dysplasia impairs hearing. (A) X-ray confirmed absent clavicles (arrows) in Runx2$^{+/-}$ and D4 mice. (B) Runx2$^{+/-}$ mice (open triangles) exhibit higher ABR thresholds than WTs (filled circles) ($^{*}P<0.001$). (C) CAP thresholds (click stimuli) were elevated in Runx2$^{+/-}$ mice. (D) Expression of Runx2 OC and nAchR-α9 mRNA in cochlear bone or soft tissue. ABR, auditory brainstem response; CAP, compound action potential; mRNA, messenger RNA; OC, osteocalcin; WT, wild type.

Although Runx2 is typically restricted to mineralizing tissues, Runx2 has also been detected in neurons (Benes et al, 2007) and its expression in the cochlea is unknown. Unlike the hair-cellspecific nicotinic acetylcholine receptor α9, Runx2 messenger RNA was expressed only in microdissected cochlear bone or in the developing cochlear capsule (Fig 2D; supplementary Fig S1 online). Runx2 was not expressed by cells that give rise to the supporting or neural structures of the cochlea, demonstrating that the effects of Runx2 haploinsufficiency on hearing loss were due to a bone-intrinsic defect.

Sensorineural structures and bone anatomy of CCD-like ears are normal

The CCD-like Runx2$^{+/-}$ and D4 mice are valuable tools to study the unexplained cause of SNHL in CCD and other bone diseases. Defects in the organ of Corti structure, hair cells, ganglion cells or other supporting cochlear structures cause SNHL. However, no differences in the sensorineural structures of the inner ear were observed in either Runx2$^{+/-}$ or D4 mice (Fig 3A,B; supplementary Fig S2 online). Together, three functional hearing tests (ABR, CAP and distortion product otoacoustic emission) localized the hearing defect to the peripheral auditory system and showed that conductive hearing remains largely intact, strongly suggesting a cochlear aetiology for hearing loss (Fig 2B,C; supplementary Fig S3 online).

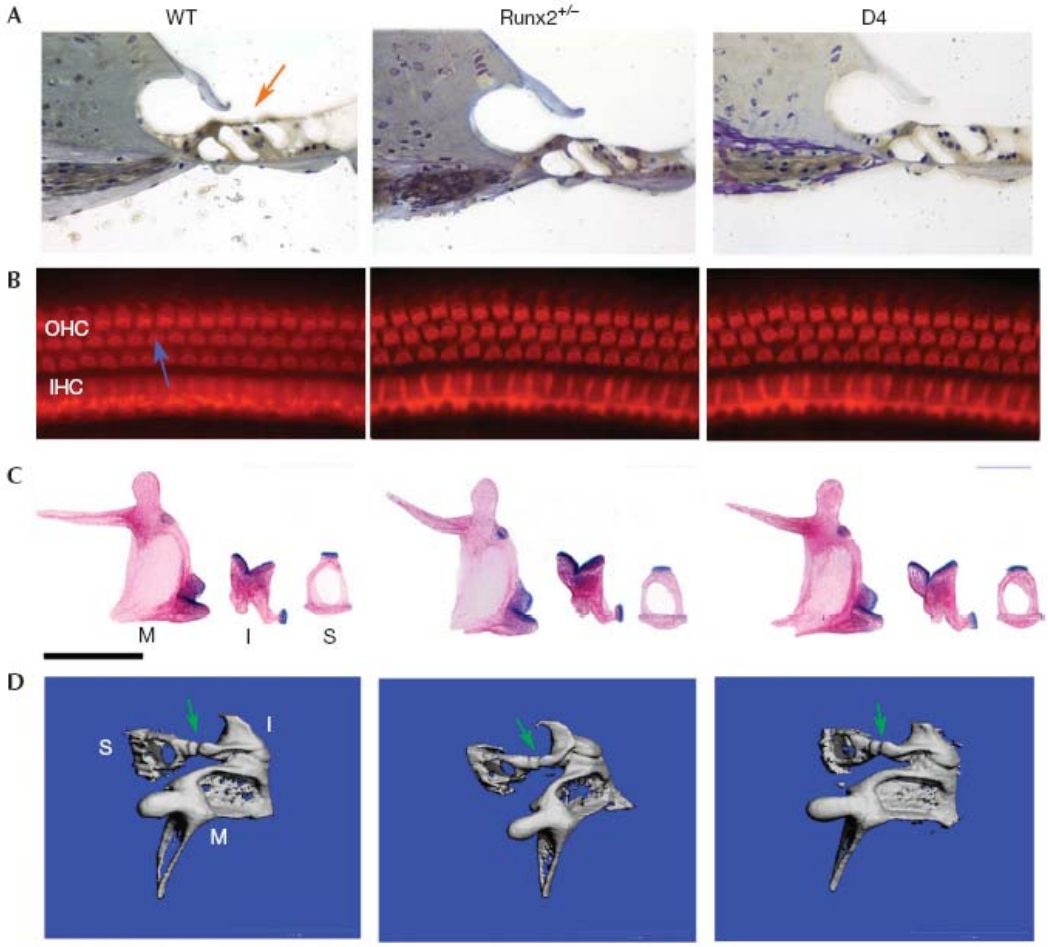

Fig 3 Mouse models of cleidocranial dysplasia lack discernible defects in cochlear structures. (A) No differences between WT, Runx2$^{+/-}$ and D4 cochleae were observed in the organ of Corti (orange arrow), spiral ligament, stria vascularis and spiral ganglia. (B) Phalloidin-stained organ of Corti showed normal organization with one IHC row and 3–4 OHC rows. Sterocilia (blue arrow) are normal in each strain. (C) Dissected ossicles (malleus (M), incus (I), stapes (S)) stained for bone and cartilage showed normal development and mineralization at 6 days of age. (D) Micro-CT shows that each ossicle and the joints (green arrow) between them are intact. Apparent differences are artefacts of imaging at scanner resolution limits. CT, computed tomography; IHC, inner hair cell; OHC, outer hair cell; WT, wild type.

As bone-intrinsic defects could cause hearing loss, we examined the outer, middle and inner ears of WT, Runx2$^{+/-}$ and D4 mice anatomically, radiologically and histologically. For example, OPG$^{-/-}$ mice exhibit gross ear bone defects, due to hyperactive osteoclasts, which cause hearing loss similar in magnitude to that in D4 and Runx2$^{+/-}$ mice (Kanzaki et al, 2006; Zehnder et al, 2006). However, our studies found no such defects (Fig 3C,D; supplementary Fig S2 online). Therefore, hearing loss in mouse models of CCD is not explained by overt developmental or anatomical defects in the skeletal or sensorineural structures of the ear.

Runx2 regulates bone matrix material properties and mineralization

Next, we sought to determine whether hearing loss in Runx2$^{+/-}$ mice was due to the altered material properties of cochlear bone. Although TGFβ regulates bone material properties (Fig 1B,C), the underlying mechanisms for this are unknown. Furthermore, a role for Runx2 or any other transcription factor in the control of ECM material properties has not been reported. Nanoindentation revealed a reduction in the hardness and elastic modulus of Runx2$^{+/-}$ cochlear bone, relative to WT (Fig 4A,B). A major determinant of bone matrix material properties is the mineral content, which can be quantified using X-ray tomography (XTM). Using XTM, a shift was shown in the distribution of mineral content of Runx2$^{+/-}$ bone matrix relative to WT mice (Fig 4C). The decreased mineralization correlated with the decreased material properties of Runx2$^{+/-}$ bone matrix and resembled the reduced mineral content in D4 bone matrix (Balooch et al, 2005). We concluded that therefore, the osteoblast transcription factor Runx2 is a crucial regulator of the material properties and mineralization of bone matrix.

Loss of cochlear bone matrix material properties accounts for HL

Loss of the distinctive hardness of cochlear bone matrix in D4 and Runx2$^{+/-}$ mice was the only observed defect that could account for hearing loss in both strains, suggesting that the unique material properties of this tissue might directly affect its function. This was confirmed by a statistical analysis that related the auditory threshold to the elastic modulus of the cochlear bone matrix for the same ear. The elastic modulus correlated with ABR thresholds at 8 kHz, such that for every 1-GPa increase in elastic modulus, ABR thresholds dropped by 1.84 dB (sound pressure level; Fig 4D; P<0.01; R^2=0.77). This relationship was independent of genotype. Therefore, the defective material properties of D4 and Runx2$^{+/-}$ bone matrix correlate significantly with hearing loss.

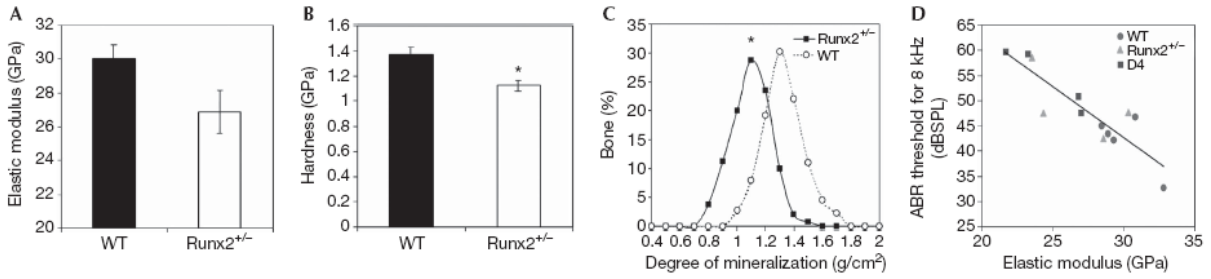

Fig 4 Cochlear bone matrix material properties are regulated by Runx2 and are essential for hearing. The (A) elastic modulus and (B) hardness of cochlear bone matrix from Runx2$^{+/-}$ mice is reduced relative to WT ($^*P$<0.01). (C) Reduced mineralization of Runx2$^{+/-}$ tibial bone as assessed by XTM. (D) Multiple linear regression analysis comparing elastic modulus with ABR thresholds for each ear shows that elastic modulus is a critical determinant of auditory function (P<0.01, R^2=0.77). ABR, auditory brainstem response; WT, wild type; XTM, X-ray tomography.

These results, to the best of our knowledge, provide the first direct evidence that ECM material properties are calibrated for their tissue-specific function. Furthermore, our results strongly suggest that changes in the specialized ear bone matrix material properties account for the unexplained SNHL in CCD. Although additional study is needed to elucidate the precise mechanisms for this, our findings might extend to hearing loss in Camurati–Engelmann disease, osteogenesis imperfecta and Paget disease, diseases which also result from defects in factors linked to bone quality (TGFβ, collagen and mineral, respectively; Higashi & Matsuki, 1996; Hartikka et al, 2004; Monsell, 2004; Balooch et al, 2005).

TGFβ represses Runx2 to regulate bone matrix material properties

The similarity of the D4 and Runx2$^{+/-}$ bone phenotypes suggests that TGFb and Runx2 act via the same pathway. In vitro, TGFβ represses Runx2 (Alliston et al, 2001). Although Runx2 mutations that ablate its binding to bone morphogenetic protein- or TGFβ-activated Smads cause CCD (Zhang et al, 2000), the regulation of Runx2 by TGFβ in vivo remains unclear. As shown in Fig 5A, TGFβ repressed the expression of the Runx2-regulated genes, osteocalcin and Runx2, by 50% in D4 calvarial bone, relative to WT. Conversely, decreased TGFβ signalling in calvariae from DNTbRII mice—which express a dominant-negative TGFβ type II receptor in osteoblasts (Filvaroff et al, 1999)—increased Runx2 and osteocalcin messenger RNA levels (Fig 5B; supplementary Fig S4 online). These results indicate that, TGFβ represses Runx2 function in vivo and in vitro.

Although transcription factors respond to growth factors in order to regulate gene expression and differentiation, their ability to control ECM material properties has not been explored. To determine whether Runx2 functions downstream from TGFβ in the control of bone matrix material properties, Runx2$^{+/-}$ mice were crossed with DNTβRII mice. We hypothesized that the Runx2$^{+/-}$ phenotype would be rescued by the inhibition of TGFb function. In DNTβRII; Runx2$^{+/-}$ mice, TGFβ inhibition did not rescue the clavicle dysplasia of Runx2$^{+/-}$ mice (Fig 5C). However, the reduced elastic modulus and hardness of Runx2$^{+/-}$ tibial bone matrix were rescued by inhibition of TGFβ signalling in osteoblasts (Fig 5D). Blocking the ability of autocrine TGFβ to repress Runx2 function was also sufficient to rescue the defective mineralization of Runx2$^{+/-}$ bone. Unmineralized patches, apparent only in Runx2$^{+/-}$ bone, were absent in DNTβRII; Runx2$^{+/-}$ bone matrix (Fig 5E). Therefore, TGFβ regulates mineralization and matrix material properties through the same pathway that it uses to control cellular differentiation (Alliston et al, 2001), by repressing the activity of the lineage-specific transcription factor Runx2.

Tissue-specific calibration of ECM material properties

We investigated the mechanisms by which the distinctive material properties of a tissue are established and linked with its physiological function. Using bone matrix as a model, we identified Runx2 as a lineage-specific transcription factor that establishes ECM material properties through the same TGFβ pathway that controls osteoblast differentiation. This role of TGFβ and Smad3 extends beyond mineralized tissues, as Smad3 also controls skin ECM properties (Arany et al, 2006). Just as TGFβ regulates Runx2 function, it regulates other lineage-specific transcription factors to directly express tissue-specific ECM proteins, which in turn might influence ECM material properties. Therefore, this study elucidates the control of bone matrix quality and the role of bone in hearing. It also suggests a new paradigm in which signalling pathways and lineage-specific transcription factors cooperate to define the functionally essential ECM material properties of a specific tissue.

METHODS

Mice. The generation and skeletal abnormalities of D4, Runx2$^{+/-}$ and DNTβII mice have been described previously (Erlebacher & Derynck, 1996; Otto et al, 1997; Filvaroff et al, 1999). Mice were bred on a B6D2 × C57/Bl6 background. WT littermates were used as controls. Procedures were approved by the University of California San Francisco Institutional Animal Care and Use Committee.

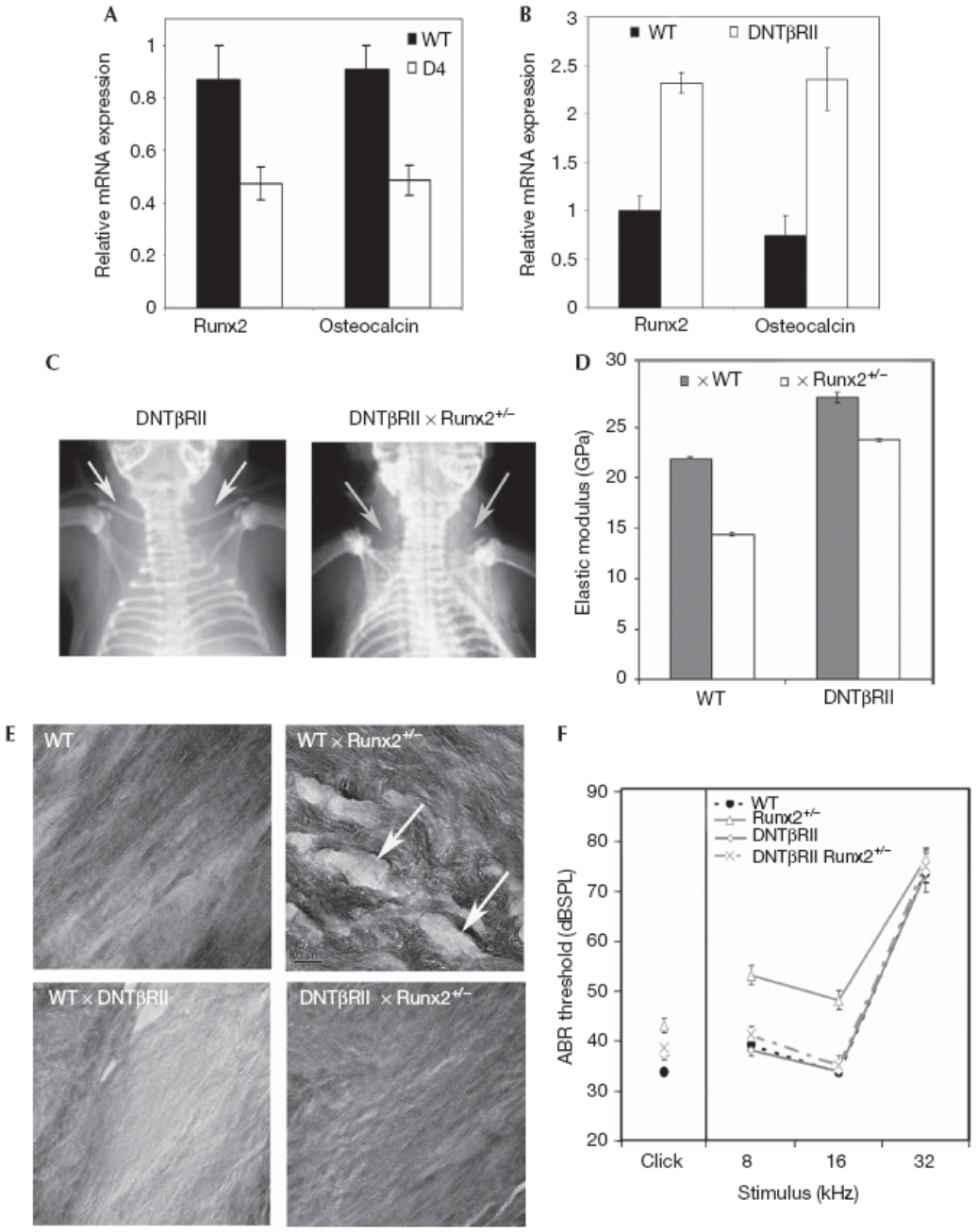

Fig 5 Defective Runx2+/- bone matrix material properties, mineralization and hearing are rescued by inhibition of transforming growth factor-β. Quantitative reverse transcriptase–PCR shows the effect of (A) elevated TGFβ in D4 mice and (B) TGFb inhibition DNTbRII mice on gene expression in calvarial bone. X-rays, nanoindentation and TEM show that (C) clavicle dysplasia is not, but (D) elastic modulus ($^{*}P<0.001$) and (E) mineralization are rescued in DNTβRII; $Runx2^{+/-}$ mice. (E) Arrows show sites lacking mineralization as detected through TEM. (F) ABR thresholds for $Runx2^{+/-}$ (open triangles), DNTβRII (asterisks) and DNTβRII; $Runx2^{+/-}$ (×), or WT mice (filled circles) are shown. ABR, auditory brainstem response; TEM, transmission electron microscopy; TGFβ, transforming growth factor-β; WT, wild-type.

Auditory function. Evoked auditory brainstem response thresholds, compound action potentials and distortion product otoacoustic emissions were measured in 2-month-old male mice (nX4; Akil et al, 2006; Seal et al, 2008). Statistical analysis used one-way analysis of variance ($P<0.05$).

Histology and analysis of gene expression. Cochlear histology studies were carried out on nX3 mice (Akil et al, 2006). Qualitative hair cell analysis was performed on dissected cochleae by microscopic visualization of rhodamine–phalloidin staining (nX3; Seal et al, 2008). Dissected ossicles from 1- and 6-day-old mice were

stained with Alizarin red and Alcian blue to visualize bone and cartilage, respectively (nX3; Otto et al, 1997). Gene expression was assessed using RNA isolated from dissected calvariae or cochlear bone or soft tissue (nX4; Seal et al, 2008; Mohammad et al, 2009). Using quantitative reverse transcriptase–PCR, amplification of Runx2, osteocalcin and nAchR-α9 were normalized to ribosomal protein L19. Statistical differences were calculated by Student's t-test ($P<0.05$).

Micro-computed tomography. Temporal bones, dissected with intact bulla to preserve the ossicular chain, were scanned by micro-computed tomography (n=3; VivaCT-40, Scanco). Image acquisition consisted of 418 slices encompassing the cochlea at 10.5-mm voxel size. For each 180°, 1,000 projections were taken. The integration time was 346, with potential of 55 kVp and current of 145 mA. The images were segmented using a low pass filter, and a threshold (0.7/1/270) was uniformly applied. For threedimensional reconstruction, cochlear bone was excluded to visualize the ossicular chain in 200–220 slices.

Nanoindentation, XTM and transmission electron microscopy. For nanoindentation, cochleae were cut along the modiolar axis with a scalpel before mounting in epoxy resin. The malleus was mounted with epoxy without cutting or polishing. Using a saw, tibiae and femora were cut to expose mid-diaphyseal cortical bone, whereas calvariae were cut sagitally. Polished sections were nanoindented in load-control by using a Nanoscope III atomic force microscope (Veeco) with a Triboscope indenter head with a Berkovich tip (Hysitron; Mohammad et al, 2009). Indentations in three 30-mm lines with a 2-mm step size were placed across the cortical bone surfaces, but near the apex of the cochlea. Malleus material properties were determined using 10 indents per bone. Loading and unloading rates were 100 mN/s with a 10-s dwell time. For each bone, calculated elastic modulus or hardness values were averaged (25,26). Statistical analysis used one-way analysis of variance ($P<0.05$). XTM and transmission electron microscopy were performed as described previously (Mohammad et al, 2009; Thurner et al, 2010).

Supplementary information is available at EMBO reports online (http://www.emboreports.org).

ACKNOWLEDGEMENTS

We thank C. Weber, D. Nguyen, D. Coling, R. Stern, G. Nonomura, L. Prentice and V. Weaver. This research was supported by Howard Hughes Medical Institute Medical Student Research Fellowship (J.L.C.), Triological Society Resident Research Fellowship (J.J.), T32 DE007306 (C.C.), Hearing Research Institute (A.L., L.L., T.A.), R01 DE016402 (R.A.S.), National Institutes of Health National Center for Research Resources (R.D.), P01 DE09859 (D.S.B., G.W.M., S.J.M.), National Institute on Deafness and Other Communication Disorders K08 DC00189 (L.L.) and University of California, San Francisco School of Dentistry Creativity Fund, Arthritis Foundation, RO3 DE16868, Deafness Research Foundation and R01 DE019284 (T.A.). X-ray tomography was performed at Advanced Light Source at Lawrence Berkeley National Laboratory (United States Department of Energy, DEAC02-05CH11231).

CONFLICT OF INTEREST

The authors declare that they have no conflict of interest.

REFERENCES

Akil O, Chang J, Hiel H, Kong JH, Yi E, Glowatzki E, Lustig LR (2006) Progressive deafness and altered cochlear innervation in knock-out mice lacking prosaposin. J Neurosci 26: 13076–13088

Alliston T, Choy L, Ducy P, Karsenty G, Derynck R (2001) TGFb-induced repression of CBFA1 by Smad3 decreases cbfa1 and osteocalcin expression and inhibits osteoblast differentiation. EMBO J 20: 2254–2272

Arany PR, Flanders KC, Kobayashi T, Kuo CK, Stuelten C, Desai KV, Tuan R, Rennard SI, Roberts AB (2006) Smad3 deficiency alters key structural elements of the extracellular matrix and mechanotransduction of wound closure. Proc Natl Acad Sci USA 103: 9250–9255

Balooch G, Balooch M, Nalla RK, Schilling S, Filvaroff EH, Marshall GW, Marshall SJ, Ritchie RO, Derynck R, Alliston T (2005) TGFb regulates the mechanical properties and composition of bone matrix. Proc Natl Acad

Sci USA 102: 18813–18818

Benes FM, Lim B, Matzilevich D, Walsh JP, Subburaju S, Minns M (2007) Regulation of the GABA cell phenotype in hippocampus of schizophrenics and bipolars. Proc Natl Acad Sci USA 104: 10164–10169

Butcher DT, Alliston T, Weaver VM (2009) A tense situation: forcing tumour progression. Nat Rev Cancer 9: 108–122

Chole RA, McKenna M (2001) Pathophysiology of otosclerosis. Otol Neurotol 22: 249–257

Cooper SC, Flaitz CM, Johnston DA, Lee B, Hecht JT (2001) A natural history of cleidocranial dysplasia. Am J Med Genet 104: 1–6

Currey JD (1999) The design of mineralised hard tissues for their mechanical functions. J Exp Biol 202: 3285–3294

Erlebacher A, Derynck R (1996) Increased expression of TGFb2 in osteoblasts results in an osteoporosis-like phenotype. J Cell Biol 132: 195–210

Filvaroff E, Erlebacher A, Ye J, Gitelman SE, Lotz J, Heillman M, Derynck R (1999) Inhibition of TGFb receptor signaling in osteoblasts leads to decreased bone remodeling and increased trabecular bone mass. Development 126: 4267–4279

Hartikka H, Kuurila K, Korkko J, Kaitila I, Grenman R, Pynnonen S, Hyland JC, Ala-Kokko L (2004) Lack of correlation between the type of COL1A1 or COL1A2 mutation and hearing loss in osteogenesis imperfecta patients. Hum Mut 24: 147–154

Higashi K, Matsuki C (1996) Hearing impairment in Engelmann disease. Am J Otol 17: 26–29

Kanzaki S, Ito M, Takada Y, Ogawa K, Matsuo K (2006) Resorption of auditory ossicles and hearing loss in mice lacking osteoprotegerin. Bone 39: 414–419

Mohammad KS et al (2009) Pharmacologic inhibition of the TGFb type I receptor kinase has anabolic and anti-catabolic effects on bone. PLoS ONE 4: e5275

Monsell EM (2004) The mechanism of hearing loss in Paget's disease of bone. Laryngoscope 114: 598–606

Otto F et al (1997) Cbfa1, a candidate gene for cleidocranial dysplasia syndrome, is essential for osteoblast differentiation and bone development. Cell 89: 765–771

Rho JY, Tsui TY, Pharr GM (1997) Elastic properties of human cortical and trabecular lamellar bone measured by nanoindentation. Biomaterials 18: 1325–1330

Seal RP et al (2008) Sensorineural deafness and seizures in mice lacking vesicular glutamate transporter 3. Neuron 57: 263–275

Sorensen MS (1994) Temporal bone dynamics, the hard way. Formation, growth, modeling, repair and quantum type bone remodeling in the otic capsule. Acta Otolaryngol 512: 1–22

Thurner PJ, Chen CG, Ionova-Martin S, Sun L, Harman A, Porter A, Ager JW III, Ritchie RO, Alliston T (2010) Osteopontin deficiency increases bone fragility but preserves bone mass. Bone 46: 1564–1573

Visosky AM, Johnson J, Bingea B, Gurney T, Lalwani AK (2003) Otolaryngological manifestations of cleidocranial dysplasia, concentrating on audiological findings. Laryngoscope 113: 1508–1514

Zehnder AF, Kristiansen AG, Adams JC, Kujawa SG, Merchant SN, McKenna MJ (2006) Osteoprotegrin knockout mice demonstrate abnormal remodeling of the otic capsule and progressive hearing loss. Laryngoscope 116: 201–206

Zhang YW, Yasui N, Ito K, Huang G, Fujii M, Hanai J, Nogami H, Ochi T, Miyazono K, Ito Y (2000) A RUNX2/PEBP2alpha A/CBFA1 mutation displaying impaired transactivation and Smad interaction in cleidocranial dysplasia. Proc Natl Acad Sci USA 97: 10549–10554